ELSEVIER

Coordination Chemistry Reviews
196 (2000) 281–305

COORDINATION CHEMISTRY REVIEWS

www.elsevier.com/locate/ccr

Photochemical reactions of amminerutheniu(II) complexes

Elia Tfouni *

Departamento de Química, Faculdade de Filosofia, Ciências e Letras de Ribeirão Preto, Universidade de São Paulo, Av. dos Bandeirantes, 3900, 14040-901, Ribeirão Preto, São Paulo, Brazil

Received 4 January 1999; received in revised form 13 May 1999; accepted 22 June 1999

Contents

Abbreviations: ACN, acetonitrile; 4-acpy, 4-acetylpyridine; bzn, benzonitrile; CT, charge-transfer; CTTS, charge-transfer to solvent; 3-Clpy, 3-chloropyridine; NCpy, cyanopyridine; 2-NCpy, 2-cyanopyridine; 3-NCpy, 3-cyanopyridine; 4-NCpy, 4-cyanopyridine; en, ethylenediamine; edta, ethylenediaminetetraacetate; IL, intra-ligand; isn, isonicotinamide; λ_{irr}, irradiation wavelength; LF, ligand field; LEES, lowest energy excited state; MLCT, metal to ligand charge-transfer; 4-mcp, 1-methyl-4-cyanopyridinium; mpz, 1-methylpyrazinium; nic, nicotinamide; 4-pic, 4-picoline; PR_3, phosphine; $P(OR)_3$, phosphite; py, pyridine; py-X, X substituted pyridine; pz, pyrazine; cyclam, 1,4,8,11-tetraazacyclotetradecane; $P(OEt)_3$, triethylphosphite; $AsPh_3$, triphenylarsine; PPh_3, triphenylphosphine; $SbPh_3$, triphenylstibine; TPA, 1,3,5-triaza-7-phosphaadamantane.

* Tel.: +55-16-602-3748; fax: +55-16-633-8151.
E-mail address: eltfouni@usp.br (E. Tfouni)

PII: S0010-8545(99)00200-3

Abstract

A survey is given of the photochemical reactions displayed by ruthenium(II)–amine complexes, except for polypyridyl complexes, and including contributions from this laboratory. The latest review on the subject dates from the early 1980s. Since then, several contributions have appeared in the literature which could be brought and discussed together, giving an updated and unified view of the subject. Spectra and the nature of the excited states relevant for the discussion are described. Reactions will be discussed by type of reaction and of complexes. The reactions will mainly focus on photosubstitution, but will also include quenched and sensitized reactions, as well as eventual photooxidation reactions.

Keywords: Photochemical reactions; Ammineruthenium(II) complexes; Photosubstitution

1. Introduction

Ruthenium chemistry experienced a great jump in development during the 1960s especially due to research performed in the laboratories of Allen and of Taube [1–3]. Improvement in the synthesis of Ru(II) and Ru(III) complexes, made them more readily available, and drew attention to their rich chemistry and spectroscopy. However, the photochemistry of ruthenium complexes was scarce, as can be seen in the 1969 monograph of Balzani and Carassiti [4], until at the very end of the 1960s, a series of fundamental papers [5] on ruthenium(II) photochemistry started to appear from the group of P.C. Ford.

Over the past 3 decades there have been a number of achievements in inorganic photochemistry both in terms of their fundamental aspects as well as application.

Looking through this literature one can see an overwhelming presence of ruthenium complexes with polypyridines, the substitution inertness of which is essential for their applications. Thus, reviews on polypyridine ruthenium photochemistry and photophysics are available [6], as are reviews and a monograph on supramolecular photochemistry, which involve assemblies of basic components, many of which are ruthenium polypyridines [7].

The pentaammine and tetraaminеruthenium(II) complexes, $Ru(NH_3)_5L^{2+}$ and $Ru(NH_3)_4LL'^{2+}$ also display a very rich photochemistry; but, in these cases, their photoreactions are dominated by substitution processes. For this reason, there is less interest in possible applications in solar energy conversion, although such components have drawn attention in terms of possible non-linear optical properties. However, the ruthenium(II) ammines have provided and continue to provide fundamental insight into the excited states reactivity of d^6 metal centers. The photochemistry of such complexes was last reviewed more than 15 years ago [8–13]. Given developments in this area since then, many in the author's laboratory, the present CCR volume on Latin American Coordination Chemistry is a timely and appropriate opportunity to review the topic once more. This non-exhaustive review will cover mostly photosubstitution reactions of ruthenium(II) ammines and some related amines and will also include quenched and sensitized reactions, as well as eventual photooxidaton reactions.

2. Spectra and excited states of ruthenium(II) complexes

Among the excited states types, the LF, MLCT, CTTS, and IL excited states are displayed by mononuclear Ru(II) species. The former two states are of major importance to the photosubstitution reactions being reviewed. The CTTS excited state properties and systems where CTTS plays a role in photochemistry have been reviewed [11].

2.1. MLCT states and spectra

The properties of the MLCT states in ruthenium(II) ammine complexes depend on the nature of the ligand L [14]. This ligand must have available empty orbitals of appropriate symmetries and energies to combine with the d_π orbitals of the ruthenium(II) center. Considering an octahedral symmetry on the Ru center, the linear combination of one d_π metal orbital and one π^* ligand orbital leads to two MO, one bonding, ψ_1, and one antibonding, ψ_4 (Fig. 1). The other two orthogonal d_π orbitals, which become ψ_2 and ψ_3, are degenerate and non-bonding. In this combination ψ_1 has more Ru d_π character, whereas ψ_4 has more L ligand π^* character. An one-electron transition from ψ_1 to ψ_4 can be viewed as a transition of an electron from an orbital having mostly metal character to an orbital having mostly L ligand character, i.e. MLCT. Similarly, transitions from ψ_2, ψ_3 to ψ_4 involve depopulation of an orbital which is more metal and less delocalized in character to an orbital mostly ligand L in character. The energy difference between ψ_1 and ψ_2, ψ_3 is the back-bonding stabilization energy.

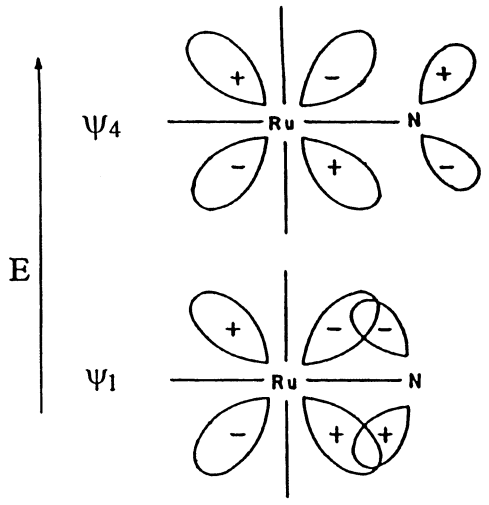

Fig. 1. Schematic molecular orbitals formed from the combination of one d_π Ru(II) orbital and one π^* orbital of the ligand L.

Fig. 2 shows a schematic MO diagram for two pentaammineruthenium(II) complexes. Fig. 2a refers to a complex with a relatively small back-bonding ability, such as pyridine. In this case at least two transitions are allowed. However, their energy difference is small, and, as a result, only one MLCT absorption band is seen in its electronic spectrum [14]. Replacing pyridine by the stronger π-acceptor ligand, mpz, resulted in $Ru^{II}(NH_3)_5(mpz)^{3+}$, which in solution displays one absorption band at 540 nm [15,16] and one at 877 nm [16]. Considering that the π^* level of mpz is lower in energy than that of py, it will match better with the d_π orbitals, and will have a higher back-bonding stabilization energy (Fig. 2b). In this situation, the transition from ψ_1 to ψ_4 will have a much higher energy than that of ψ_2, ψ_3 to ψ_4, relative to the py complex. The energy difference gives rise to two absorption

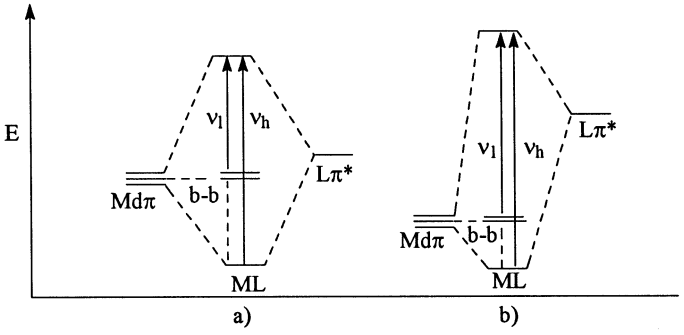

Fig. 2. Schematic molecular orbitals diagram for Ru(II)–L. (a) L is a strong π-acceptor ligand, such as mpz. (b) L is a weaker π-acceptor ligand, such as pyridine. (Figure drawn after Ref. [16].)

bands, the one at 540 nm, corresponding to the former transition, and the one at 877 nm, corresponding to the latter. Accordingly, the high energy transition involves orbitals with more covalent character, while the low energy would be a genuine MLCT [16]. The assignments were also based on the solvatochromic behavior of the low energy band, while the higher one (540 nm) is solvent insensitive.

In several papers published before 1987 (Refs. [8–13], and Refs. therein) it was accordingly assumed that MLCT would correspond to a process which involves oxidation of the ruthenium(II) center and reduction of the ligand. Formally, a MLCT transition could then be conceived as being

$$(NH_3)_5Ru^{II}\text{–}L \underset{MLCT}{\overset{h\nu}{\rightarrow}} (NH_3)_5Ru^{III}\text{–}L^- \quad (1)$$

The experimental results of the earlier research were consistent with such an assumption. Noteworthy, in 1987, the $(NH_3)_5Ru^{III}$–(py^-) transient was directly observed [17] experimentally upon irradiation of $(NH_3)_5Ru^{II}$–(py) on the MLCT state, confirming the previous assumption.

Tables 1–5 list some electronic absorption and quantum yields data of some ruthenium(II) complexes. The energy of the MLCT band is very sensitive to the nature of the ligands (Tables 1–5). In $Ru^{II}(NH_3)_5L^{n+}$ complexes with L = py-X or pz, the energy of the MLCT band varies with the nature and to the position of the substituent X on the aromatic heterocycle [14]. Electron-donating X groups destabilize Ru^{III}–$(py\text{-}X)^-$, while electron withdrawing X groups stabilize this form. Accordingly, the MLCT band which appears at 407 nm for $Ru(NH_3)_5(py)^{2+}$ is blue shifted to 398 nm by replacing H for CH_3 in the position 4 of the ring to give $(NH_3)_5Ru(4\text{-pic})^{2+}$ [18]. This same band is red shifted to 528 nm in $Ru(NH_3)_5(4\text{-acpy})^{2+}$ by replacing –H for the electron-withdrawing $–COCH_3$ group. In $Ru(NH_3)_5(py\text{-}X)$, the energy shifts of the MLCT bands are higher when the substitution is at position 4 [14].

One of the consequences of back-bonding is to make the different ligand L more basic. This can be clearly seen in the acid–base behavior of $Ru(NH_3)_5(pz)^{2+}$, which can be reversibly protonated to $Ru(NH_3)_5(pzH)^{3+}$ [14].

$$(NH_3)_5Ru(pzH)^{3+} \overset{K_a}{\rightleftharpoons} (NH_3)_5Ru(pz)^{2+} + H^+ \quad (2)$$

Protonation of the coordinated pz red shifts the MLCT band from 472 to 529 nm, enabling the spectrophotometric determination of the pK_a as 2.6, two orders of magnitude higher than that of the free pz (0.6) [14]. In comparison, the isoelectronic Rh(III) complex, $Rh(NH_3)_5(pz)^{3+}$, which lacks back-bonding, shows the coordinated pz more acidic than the free pz. In *trans*-$Ru^{II}(NH_3)_4(L)(pz)$ (L = 4-pic, py, isn, pz, or 4-acpy), the L and pz ligands compete for the electron-withdrawing from the d_π orbitals, and hence the different electron-withdrawing capability of the L ligands will be reflected in different pK_a values for the coordinated pz. The more electron-withdrawing L is the more acidic the coordinated pz and thus a smaller pK_a results [21,28]. A similar situation also holds for the ruthenium(II) ammine complexes with cyanopyridines [29,30]. Again, the coordinated cyanopyridine is more basic than the free ligand. Consequently, in systems like those, the MLCT energy can be varied by controlling the acidity of the medium.

Table 1
Photosubstitution quantum yields and some electronic absorption data of some $[Ru^{II}(NH_3)_5L]^{n+}$ complexes in aqueous media

L	λ_{max}	λ_{irr}	ϕ_{NH_3} (10^{-3})	ϕ_L (10^{-3})	ϕ_{ox} (10^{-3})	ϕ_{total}	Ref.
py	407 (MLCT)	366	43 ± 2				[18]
		405	45 ± 2	63 ± 5		108	
		436	51 ± 2				
		449	49 ± 1	63 ± 1		112	
isn	479 (MLCT)	405	4.5 ± 0.1	22 ± 2		27	[18]
		449	1.5 ± 0.1				
		479	1.07 ± 0.04	5.3 ± 0.2		6.4	
		500	0.37 ± 0.02	2.4 ± 0.1		2.8	
		520	0.35 ± 0.02				
		546	0.30 ± 0.02	0.7 ± 0.1		1.0	
pz	472 (MLCT)	479	1.4 ± 0.1	1.8 ± 0.2		3.2	[18]
4-acpy	523 (MLCT)	405	4.5 ± 0.7	27 ± 1		32	[18]
		449	1.4 ± 0.1	8.6 ± 0.5		10	
		520	0.25 ± 0.06	0.9 ± 0.1		1.2	
2-NCpy	406 (MLCT)	365	71 ± 1	56 ± 2		127 ± 3	[19]
		404	72 ± 2	40 ± 1		112 ± 3	
		436	65 ± 2	58 ± 1		123 ± 3	
4-NCpy	424 (MLCT)	365	16 ± 1	37 ± 1		51 ± 2	[19]
		404	18 ± 1	35 ± 2		53 ± 3	
		436	16 ± 1	28 ± 1		44 ± 2	
acn	226 (MLCT)	213.9	<40	<30	510 ± 60		[20]
	350 (LF)	228.8	<30	<30	380 ± 90		
		254	120 ± 10		160 ± 10		
		313	130 ± 10	100 ± 20	8 ± 1		
		366	160 ± 10	100 ± 20	<1		

Other very important property of the MLCT state is its solvatochromic behavior. The energies of the MLCT bands depend on the solvent used. In ruthenium(II) ammine complexes this dependence was explained by use of a model based on observations made on the solvent effects on several rutheniumammine complexes [31]. This model claims that specific solvent interactions between coordinated ammonia and the donor properties of the solvent change the redox asymmetry within the molecule (estimated as $\Delta E_{1/2} = E_{1/2}(Ru^{II}/Ru^{III}) - E_{1/2}(L/L^-)$) and that this is the main contributor to the change observed in the CT band energies. The origin of the solvent effect was described by a microscopic interaction between the solvent donor and the nitrogen-bound hydrogen atoms of the ammines. This model was based on observations that (a) plots of E_{MLCT} versus DN (Guttmann's donor number) are linear for Ru(II) ammine complexes and that the slopes for these cationic Ru(II) complexes are negative; (b) plots of $\Delta E_{1/2}$ versus DN for $Ru^{II}(NH_3)_5(4\text{-mcp})^{3+}$ are also linear; (c) plots of E_{MLCT} versus $\Delta E_{1/2}$ are linear.

Furthermore, later results using several emissive substituted tris(bipyridine)-ruthenium(II) complexes showed that $E_{1_{MLCT}}$ correlates well with $\Delta E_{1/2}$, and, more, that $E_{3_{MLCT}}$ correlates even better with $\Delta E_{1/2}$. This is noteworthy, since, in general, in non-emissive systems the energy of ^{3}MLCT should be estimated, and now this can, in principle, be checked out by measuring $\Delta E_{1/2}$.

The MLCT excited-states of $Ru^{II}(NH_3)_5L$ (L = py-X or pz) have lifetimes that vary from < 20 to ca. 450 ps in water at ca. 25°C [17] and are five orders of magnitude more basic than the ground state for the $Ru^{II}(NH_3)_5(py)$ and $Ru^{II}(NH_3)_5(pz)$ complexes [17]. Since the transient is formally $Ru^{III}(L^-)$, substitution reactions are not expected to occur as Ru(III) is known to be even more substitution inert than is Ru(II). On the other hand the $Ru^{III}(L^-)$ transient may undergo electron transfer from another substrate to the oxidized metal center [32,33] or display reactivity characteristic of the radical ligand [11], although any such reactivity may be attenuated by its very small lifetime.

$Ru^{II}(NH_3)_5L$ complexes generally display only one MLCT band [14]. However, it is possible that this band contains more than one transition [14,21]. *Cis*-tetraammineruthenium(II) complexes with two monodentate unsaturated ligands, such as azines, show two absorptions in the visible region [24,34,35], as is the case for the *cis* complexes with bidentate ligands, such as 2-substituted pyridines [36,37]. The *trans* complexes *trans*-$Ru^{II}(NH_3)_4LL'$ usually show two bands when L = L′, with the higher energy band, MLCT-2, being much less intense than the lower energy one, MLCT-1 [21]. For L = L′, MLCT-2 becomes even weaker or absent [21].

Table 2
Photosubstitution quantum yields and some electronic absorption data of some *trans*-$[Ru^{II}(NH_3)_4LL']^{n+}$ complexes in aqueous media

L	L′	λ_{max} (nm)	λ_{irr} (nm)	ϕ_L (10^{-3})	$\phi_{L'}$ (10^{-3})	ϕ_{NH_3} (10^{-3})	ϕ_{total}	Ref.
py	py	423 (MLCT)	405	28 ± 2		50 ± 14	78 ± 16	[21]
			449	25 ± 2		41 ± 2	66 ± 4	
py	pz	348 (MLCT2)	366	1.7 ± 0.3	4.3 ± 0.8	34 ± 4	40 ± 5	[21]
		474 (MLCT1)	479	0.10 ± 0.01	0.5 ± 0.1	3.6 ± 0.4	4.2 ± 0.5	
py	4-acpy	366 (MLCT2)	366	1.4 ± 0.3	1.7 ± 0.6	40 ± 5	43 ± 6	[21]
		508 (MLCT1)	520	< 0.05	< 0.05	1.0 ± 0.1	1.0 ± 0.1	
isn	NO	230 (MLCT)	310		40			[23]
		268 (LF, isnIL)	370		9			
		323 (LF)						
		486 (NO MLCT; $L \rightarrow \pi^*_{NO}$)						

Table 3
Photosubstitution quantum yields and some electronic absorption data of some *cis*-$[Ru^{II}(NH_3)_4LL']^{n+}$ complexes in aqueous media [a,b]

L	L′	λ_{max} (nm)	λ_{irr} (nm)	ϕ_L (10^{-3})	$\phi_{L'}$ (10^{-3})	ϕ_{NH_3} (10^{-3})	ϕ_{total}
py	py	366 (MLCT2)	313	32 ± 3		53 ± 4	85 ± 7
		407 (MLCT1)	365	28 ± 3		53 ± 5	81 ± 8
			405	26 ± 4		57 ± 4	83 ± 8
			436	32 ± 1		66 ± 3	98 ± 4
4-acpy	4-acpy	442 (MLCT2)	365	5.4 ± 0.6		39 ± 1	44 ± 2
		518 (MLCT1)	405	3.8 ± 0.2		30 ± 1	34 ± 1
			436	3.7 ± 0.2		9.7 ± 0.3	13.4 ± 0.5
			480	1.3 ± 0.1		3.6 ± 0.2	4.9 ± 0.3
			519	0.55 ± 0.05		1.2 ± 0.1	1.7 ± 0.1
isn	isn	413 (MLCT2)	313	9.0 ± 1		30 ± 1	39 ± 1
		478 (MLCT1)	365	8.5 ± 0.1		29 ± 1	38 ± 1
			405	7.8 ± 0.1		26 ± 1	34 ± 1
			436	2.4 ± 0.1		10 ± 1	12 ± 1
			480	1.5 ± 0.1		4.5 ± 0.3	6 ± 0.4
isn	py	378 (MLCT2)	365	3.0 ± 0.2	12.5 ± 0.4	11.5 ± 0.5	27.0 ± 1
		466 (MLCT1)	405	2.5 ± 0.1	9.7 ± 0.7	9.5 ± 0.4	22.0 ± 1
			436	2.5 ± 0.1	8.4 ± 0.2	8.2 ± 0.1	19.1 ± 0.4
			480	1.1 ± 0.1	3.8 ± 0.1	3.8 ± 0.1	8.7 ± 0.3
isn	4-acpy	426 (MLCT2)	365	4.8 ± 0.1	1.1 ± 0.1	9.7 ± 0.1	15.6 ± 0.3
		503 (MLCT1)	405	2.6 ± 0.1	0.9 ± 0.1	6.2 ± 0.1	9.7 ± 0.3
			436	2.2 ± 0.1	0.7 ± 0.1	5.0 ± 0.1	7.9 ± 0.3
			480	0.7 ± 0.1	0.04 ± 0.01	1.3 ± 0.1	2.0 ± 0.2
			519	$< 0.4 \pm 0.1$	< 0.01	0.7 ± 0.1	$< 1.1 \pm 0.2$

[a] pH ca. 4.
[b] Ref. [24].

2.2. LF states and spectra

The spectra of ammineruthenium(II) complexes with unsaturated ligands are dominated by broad, high intensity ($\varepsilon = 10^4$ M^{-1} cm^{-1}), MLCT absorption bands in the UV–vis region, generally covering the presence of much weaker LF bands [18,21,24,34,35]. Considering that the photosubstitution behavior being covered in this review is claimed to come from LF excited states, then it is photochemically important to locate the LF bands in such complexes.

Hexaammineruthenium(II) is a d^6 low-spin octahedral species, and its UV–vis spectrum in water displays its lowest energy LF band assigned as a $^1T_{1g} \leftarrow {}^1A_{1g}$ transition at 390 nm [38,39]. There is a higher energy band at 275 nm with a barely discernible shoulder at 310 nm. In 80% aqueous ethanol the higher energy band is shifted to 264 nm and the shoulder at 310 nm becomes more resolved. The 310 nm LF band was assigned to a $^1T_{2g} \leftarrow {}^1A_{1g}$ transition, while the higher energy band

Table 4
Electronic absorption data and photosubstitution quantum yields of some *trans*-$[Ru^{II}Cl(cyclam)L]^{n+}$ complexes in aqueous media [a,b]

L	λ_{max}	λ_{irr}	ϕ_L (10^{-3})
4-pic	340 (LF)	365	25 ± 1
	390 (MLCT)	404	21 ± 3
		436	20 ± 2
py	326 (LF)	365	20 ± 3
	405 (MLCT)	404	16 ± 1
		436	21 ± 3
		480	18 ± 2
isn	345 (LF)	365	6 ± 0.6
	480 (MLCT)	480	5 ± 0.5
4-acpy	350 (LF)	365	<1
	520 (MLCT)	520	<1

[a] pH ca. 4.
[b] Ref. [25].

would be a CTTS [39]. $Co(NH_3)_6^{3+}$, which is also an octahedral d^6 low-spin complex, displays its lowest energy LF band assigned as a $^1T_{1g} \leftarrow {}^1A_{1g}$ transition at 472 nm [40]. $Co(NH_3)_5py\text{-}X^{3+}$ (py-X = py; nic; or isn) do not show MLCT bands and they all display its lowest energy LF band near 472 nm [41]. In addition, the octahedral d^6 low-spin complex $Rh(NH_3)_6^{3+}$, which is isoelectronic with Ru(II), shows its lowest energy LF band, assigned to the $^1T_{1g} \leftarrow {}^1A_{1g}$ transition, at 305 nm [42]. Again, the d^6 low-spin complexes $Rh(NH_3)_5py\text{-}X^{3+}$ (py-X = py; 4-pic; or 3-Clpy), which, as $Co(NH_3)_5py\text{-}X^{3+}$, do not display MLCT bands in their UV–vis spectra, show their lowest energy LF bands at ca. 302 nm in their UV–vis spectra

Table 5
Photosubstitution quantum yields and some electronic absorption data of some *trans*-$[Ru^{II}(NH_3)_4LL']^{2+}$ (L = $P(OR)_3$ or PR_3; L′ = $P(OR)_3$, PR_3, H_2O, or CO) complexes in aqueous media

L	L′	θ [a]	λ_{max} (nm)	λ_{irr} (nm)	$\phi_{L'}$ (10^{-3})	ϕ_{NH_3} (10^{-3})	Ref.
$P(OEt)_3$	CO	109	284 (LF)	313	70 ± 1	270 ± 30	[26,27]
$P(OEt)_3$	$P(OEt)_3$	109	260; 297 (LF)	313	40 ± 3	300 ± 20	[22]
			359 (LF)	370	<1	270 ± 40	
$P(OEt)_3$	H_2O	109	316 (LF)	313		340 ± 60	[22]
			390 (LF)	390		300 ± 40	
$P(O^iC_4H_9)_3$	$P(O^iC_4H_9)_3$	172	262; 294 (LF)	313	67 ± 4	340 ± 30	[22]
$P(O^iC_4H_9)_3$	H_2O	172	316 (LF)	313		360 ± 30	[22]
$P(O^iC_3H_7)_3$	$P(O^iC_3H_7)_3$	130	262; 294 (LF)	313	44 ± 3	310 ± 20	[22]
$P(O^iC_3H_7)_3$	H_2O	130	316 (LF)	313		350 ± 20	[22]

[a] P(III) ligand cone angle in degrees, from Ref. [22].

[42]. The nitrile bonded $[Co(NH_3)_5L]^{2+}$ (L = 2-NCpy, 3-NCpy, or 4-NCpy) display LF bands in the 469–475 nm range in their UV–vis spectra [43]. Therefore, given such evidence, py-X and NCpy are considered to have the same ligand field strength as ammonia. Hence, although not observed, the lowest energy LF band of $Ru^{II}(NH_3)_5(L)$ and $Ru^{II}(NH_3)_4(L)(L')$ (L = py-X or NCpy) have been considered to lie at ca. 390 nm.

Despite the large number of ruthenium(II) complexes with hidden LF bands, there are some examples of ruthenium amine complexes displaying LF bands in their UV–vis spectra [22,26,27,29,44–46]. In contrast to MLCT bands, LF band energies are rather insensitive to solvent, although in some instances, where the first coordination sphere is perturbed, solvatochromism of the LF band may occur. Although the MLCT excited state was observed, the LF* band was not, and it was inferred that it should have a shorter life-time than the MLCT* which is in the ps range [17].

Ruthenium(II) is generally hexacoordinate and low-spin in its complexes. Assuming a parental octahedral symmetry, as in $Ru(NH_3)_6^{2+}$, LF transitions involve depopulation of the π symmetry t_{2g} orbitals and population of the σ^*e_g orbitals, making the ligands more prone to lability. Hence, ligand substitution may be expected from LF excited states. Furthermore, in complexes with back-bonding ligands such as pyridines, nitriles, phosphites, CO, not only e_g population is important in the photosubstitution process, but depopulation of certain $t_{2g}d_\pi$ orbitals is also important as we shall see later.

3. General aspects of the photochemical behavior of Ru(II) amine complexes

The ammine complexes of ruthenium(II) can be classified into two types. Those with saturated ligands, such as ammonia, water, and ethylenediamine, have no MLCT excited state, and the lowest energy excited state (LEES) is LF in character; at higher energies, a CTTS excited state may also be present. The other type is constituted by complexes which have at least one unsaturated ligand leading to the presence of MLCT excited states in addition to the former two; the energy of these MLCT states may be higher or lower than that of the LF states. Preliminary reports on $Ru(NH_3)_5(N_2)^2$ and $(NH_3)_5Ru(N_2)Ru(NH_3)_5^{4+}$ [47]; $Ru(NH_3)_5(py)^{2+}$, $Ru(NH_3)_5(acn)^{2+}$, $Ru(NH_3)_5(OH_2)^{2+}$, and $Ru(NH_3)_6^{2+}$ [5a] showed that irradiation with UV–vis light leads the former two complexes to photooxidation processes, whereas the latter four show photooxidation and photosubstitution reactions. These systems were further examined, as we shall see. The photosubstitution reactions observed for the ruthenium(II) pentaammines and tetraammines can be schematically seen in the following reactions:

$$[Ru(NH_3)_4LL']^{2+} \xrightarrow[H_2O]{h\nu} \begin{cases} \xrightarrow{a} [Ru(NH_3)_4(H_2O)L']^{2+} + L \\ \xrightarrow{b} [Ru(NH_3)_4L(H_2O)]^{2+} + L' \\ \xrightarrow{c} [Ru(NH_3)_3(H_2O)LL']^{2+} + NH_3 \end{cases} \quad (3)$$

3.1. Ru(II) amine complexes with saturated ligands

These systems have been fully discussed [5a,11,48] and will be mentioned only briefly here.

The simplest system studied, without a doubt, is $Ru(NH_3)_6^{2+}$ [5a,48]. The UV–vis spectrum of the aqueous solution of this complex shows two LF absorption bands at 390 and 310 nm and a CTTS absorption band at 275 nm [39]. Photolysis of this complex in aqueous solutions leads to two independent, primary photoreactions: ammonia aquation and oxidation of Ru(II) to Ru(III) with concomitant formation of H_2 [5a,48]. Irradiation at longer wavelengths (313–405 nm), corresponding to LF population, leads predominantly to photoaquation with irradiation wavelength-independent quantum yields ($\phi_{aq} = 0.26 \pm 0.1$ mol einstein^{-1}). Irradiation wavelength-independent photooxidation quantum yields are also observed at this lower energy range, and it is argued that it is the result of the back-population from a common LF state into a higher energy CTTS state. For $\lambda_{irr} < 313$ nm, an increase in ϕ_{ox} and a simultaneous decrease in ϕ_{aq} are observed. Similar features were observed in the photolysis of aqueous solutions of $Ru(NH_3)_5(OH_2)^{2+}$ [5a,48]. However, ammonia photoaquation was not observed in this complex, and the spectroscopically undetectable water photolabilization was not examined by other techniques [48].

The same general features observed in the photolysis of $Ru(NH_3)_6^{2+}$ and $Ru(NH_3)_5(OH_2)^{2+}$ occur for $Ru(en)_3^{2+}$, with some particular differences [48]. The primary photoprocesses, photooxidation and photoaquation, lead to $Ru(en)_3^{3+}$ and $Ru(en)_2(enH)(OH_2)^{2+}$ as photoproducts [48].

3.2. Ru(II) amine complexes with unsaturated ligands

3.2.1. Molecular nitrogen complexes

The study of the photochemistry of ruthenium(II) ammine complexes started in 1969 with this class of complexes [5a,49]. We will begin by focusing on $Ru(NH_3)_5(N_2)^{2+}$. The UV–vis spectrum of aqueous solutions of this complex shows absorption bands at 222 nm ($\varepsilon = 1.65 \times 10^4$) and at 262 nm ($\varepsilon = 615$) [49]. Preliminary qualitative experiments showed that irradiation of aqueous solutions of $Ru(NH_3)_5(N_2)^{2+}$, and of this complex in the presence of $(NH_3)_5Ru(N_2)Ru(NH_3)_5^{4+}$, with unfiltered lights from either low or high-pressure mercury lamps results in oxidation of the complex, but the oxidizing species was not identified, although N_2 reduction was suggested [47]. Later examination [20] of the mononuclear species showed that irradiation of acidic (pH 2 and 3) aqueous solutions of the complex with 254 nm light leads to photooxidation as the main primary photochemical step, with the formation of H_2. Formation of minor quantities of $Ru(NH_3)_5(OH_2)^{2+}$ was inferred from the proposed mechanism of the reactions [20].

3.2.2. The tuning model. Ru(II) pentaammines with azines, pyrazine, or nitriles

3.2.2.1. $Ru(NH_3)_5(py)^{2+}$. The UV–vis spectrum of an aqueous solution of $Ru(NH_3)_5(py)^{2+}$ shows a MLCT band at 408 nm ($\varepsilon = 7800$) and a ligand π–π^*

band at 244 nm ($\varepsilon = 4570$) [14]. Preliminary results [5a], showed that irradiation of solutions of this complex with visible light of energy corresponding to the MLCT band (408 nm) leads to ligand photoaquation, and irradiation with UV light also results in photooxidation of the complex with the formation of molecular hydrogen. Further examination of this complex showed that irradiation with light of wavelength 366, 405, and 436 nm leads to pyridine and *cis* and *trans* ammonia photoaquation as the major photochemical pathways [5b,5c,50]. In addition, quantum yields for pyridine photoaquation were pH dependent [5b,5c,50] ranging from ca. 0.04 mol einstein^{-1} at high pH (8.1) to ca. 0.12 mol einstein^{-1} at low pH (0.2 M HCl), being ruthenium concentration dependent at very low pH values, with the ammonia photoaquation quantum yield being apparently pH insensitive. The $Ru(NH_3)_5(4\text{-pic})^{2+}$, also showed pH dependent 4-pic photosubstitution quantum yields, whereas $Ru(NH_3)_5(3\text{-Clpy})^{2+}$ did not show such dependence [5c,50]. Irradiation of $Ru(NH_3)_5(py)^{2+}$ with UV light (334, 313, 303, and 253.7 nm) led both to photoaquation and photooxidation of the complex [20]. The constant value found for ϕ_{py} suggested that excitation into upper states, including π–π^* internal ligand excited state, is followed by relatively efficient interconversion to a lower energy common excited state. Despite the relatively constant ϕ_{py}, a photoredox process occurs from an upper excited state. Since molecular hydrogen is a reaction product, a CTTS state was claimed to be responsible for the photooxidation pathway, which apparently does not provide a dominant alternative mechanism for nonradiative deactivation directly to the ground state.

The pH dependent pyridine photosubstitution quantum yields for $Ru(NH_3)_5(py)^{2+}$ were explained by the formation of a η^2-bonded py-Ru(II) intermediate. A relatively long-lived intermediate was also detected giving further support to this hypothesis [33].

3.2.2.2. $Ru(NH_3)_5L^{2+}$. (L = py-X; pz) and the excited-state tuning model [10–13,18]. Irradiation of acidic (pH 3.0) aqueous solutions of these complexes, with light of energy encompassing that of the MLCT absorption band, led to ammonia and py-X and pz photoaquation, with larger quantum yields for ammonia aquation [18], as schematized in Eq. 4:

$$[Ru(NH_3)_5(py\text{-}X)]^{2+} \xrightarrow[H^+,\,H_2O]{h\nu} \begin{cases} [Ru(NH_3)_5(H_2O)]^{2+} + py\text{-}X \\ [Ru(NH_3)_4(H_2O)(py\text{-}X)]^{2+} + NH3 \end{cases} \quad (4)$$

The rather large number of complexes examined and the characteristic broadness of the CT bands, allowed some observations concerning their photochemistry that lead to the formulation of the excited-state tuning model [10–13,18].

The $Ru(NH_3)_5(py\text{-}X)^{2+}$ and $Ru(NH_3)_5(pz)^{2+}$ complexes were classified in terms of their quantum yields. The 'reactive' complexes are those with relatively high, wavelength-independent, quantum yields, and with MLCT $\lambda_{max} \leq 460$ nm; the

'unreactive' complexes, are those with relatively low, wavelength-dependent quantum yields, with $\lambda_{max} \geq 460$ nm. This behavior was explained in terms of a 'tuning model' [10–13,18]. As was said, substitution reactions can be expected from LF excited states (LF*). Now, assuming that LF bands in these complexes lie at ca. 390 nm, and should be hidden by the much more intense MLCT bands, especially those around 390 nm, it was proposed that the excited state(s) responsible for the photosubstitution observed have LF character. Thus, the 'reactive' complexes have a LF state as the LEES, while the unreactive have a MLCT state as the LEES. The 'unreactive' complexes are three orders of magnitude less photosubstitution labile when irradiated at the MLCT λ_{max}. Since in contrast to LF, the MLCT λ_{max} depends on the nature of the substituent X in py-X, variation of X alone is capable of 'tuning' the energies of the MLCT excited states. This determines the nature of the LEES as LF* or MLCT*, and as a consequence as 'reactive' or 'unreactive' complexes, respectively.

According to the 'tuning model' [10–13,18], for 'reactive complexes' initial excitation into the MLCT* manifold is followed by relatively efficient interconversion to the lowest energy LF* from which deactivation pathways lead to aquation products or the starting complex. A reasonable pathway for the deactivation from the initial excitation would be a relatively efficient decay to the lowest MLCT* followed by crossing into the LF* manifold. The relative wavelength independence of the quantum yields for the 'reactive' complexes implies more efficient interconversion to a common state, not disregarding a possible role of some upper excited states, presumably LF* in character. The 'unreactive' complexes would have a MLCT* as LEES, and, so, any ligand aquation would come from higher energy LF states. Initial excitation into the MLCT manifold is followed by deactivation to the lowest energy MLCT* competitive with crossing into the LF* manifold.

Fig. 3 shows a schematic Jablonski diagram for *cis*-$[Ru(NH_3)_4LL']^{2+}$ complexes, which have two MLCT bands in their spectra [24]. For the pentaammines, the diagram is similar to that one, except that it has only one MLCT [18]. The diagram illustrates the deactivation pathways for ruthenium(II) ammines with exclusive photosubstitution reactions. Referring back to the pentaammines, if deactivation to the LEES is efficient, these complexes should, thus, be much less substitution reactive than the complexes that have LF* as LEES. This is supported by the relatively low values of the quantum yields of the 'unreactive' complexes [10–13,18], which dramatically decrease with longer irradiation wavelengths. The lowest energy LF* excited state was suggested to have a $(d_{yz})^2(d_{xy})^2(d_{xz})^1(d_{z^2})^1$ electronic configuration under C_{2v} symmetry. Some of the above complexes had their photoreactivity examined in some solvents and, qualitatively, the same reaction patterns were observed [18]. The overall photolability was solvent dependent, presumably because of differences in reaction and decay rates. However, since the MLCT energy is solvent dependent, in cases where the MLCT and LF states are close in energy, a change in solvent could reverse their energetic order, and, thus, change their reactivity [18]. This tuning model was observed to apply for other d^6 low spin octahedral systems [12,51].

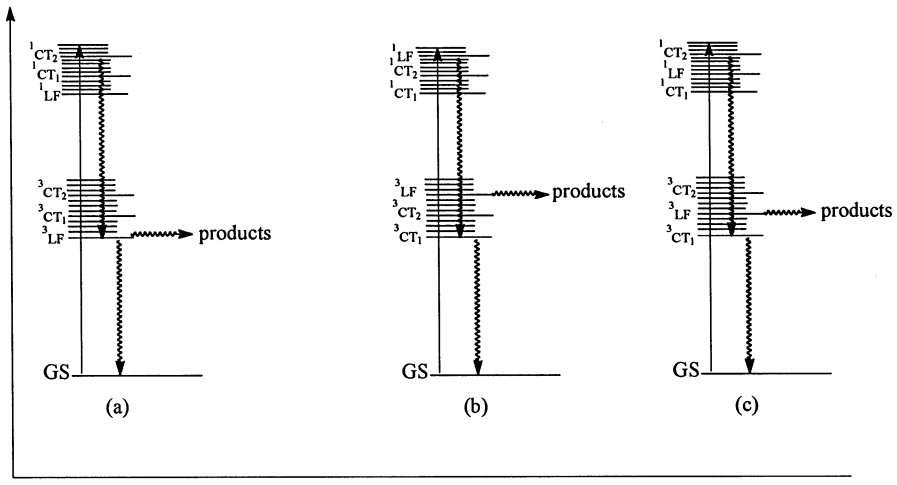

Fig. 3. Simplified Jablonski diagrams for *cis*-$[Ru(NH_3)_4LL']^{2+}$ complexes. (a) 'Reactive' complexes; (b) and (c) 'unreactive' complexes.

3.2.2.3. $Ru(NH_3)_5(acn)^{2+}$. Photoaquation and photooxidation were found to be the major photochemical pathway for $Ru(NH_3)_5(acn)^{2+}$ [5a,20]. The UV–vis spectrum of an aqueous solution of $Ru(NH_3)_5(acn)^{2+}$ shows a MLCT absorption band at 226 nm ($\varepsilon = 15\,400$), with a shoulder at 290 nm ($\varepsilon = 747$) [52] assigned as LF + CT, and a LF band at 350 nm ($\varepsilon = 163$). Ligand-field excitation with 366 nm light leads exclusively to substitution reactions with acetonitrile and ammonia photoaquation occurring with quantum yields of 0.16 and 0.10 mol einstein^{-1}, respectively, for an overall photosubstitution quantum yield of 0.26 mol einstein^{-1} [20]. Higher energy irradiation leads, in addition to photosubstitution, to photoredox products including Ru(III) species and H_2 formation. Quantum yields of Ru(III) formation increase at shorter irradiation wavelengths, with concomitant decrease of the overall substitution quantum yield. The photosubstitution reactions were claimed to originate from LF excited states as the LEES, and the photoredox processes from CTTS excited states of higher energy, forming a photochemical pattern which can be explained by competitive population of the LF and CT manifolds which do not interconvert rapidly. This situation is similar to that observed for the $Ru(NH_3)_6^{2+}$ complex.

3.2.2.4. $Ru(NH_3)_5(bzn)^{2+}$. The UV–vis spectrum of an aqueous solution of $Ru(NH_3)_5(bzn)^{2+}$ shows a MLCT band at 376 nm ($\varepsilon = 8500$), with a shoulder at 347 nm ($\varepsilon = 6900$), and IL bands at 249 nm ($\varepsilon = 16\,200$) and 226 nm ($\varepsilon = 14\,800$) [29]. Irradiation of aqueous solutions of this complex with light of 366 nm lead to benzonitrile photoaquation with quantum yields independent of pH in the range 1.0–8.89 [5b,5c,50], in contrast with the pH dependent behavior of the quantum yields of some pyridinepentaammine complexes.

3.2.2.5. $[Ru(NH_3)_5L]^{2+}$. (L = 2-NCpy, 3-NCpy, or 4-NCpy) [19]. These complexes display MLCT bands as their lowest energy bands ($\lambda_{max} = 400$ nm (3-NCpy), 406 nm (2-NCpy), and 424 nm (4-NCpy). The LF bands were estimated to be at ca. 390 nm, obscured by the MLCT bands. Irradiation with light of wavelength 365, 404, or 436 nm, at pH ca. 4.5 lead exclusively to ammonia and NCpy aquation with irradiation wavelength independent quantum yields (Eqs. 5a and 5b).

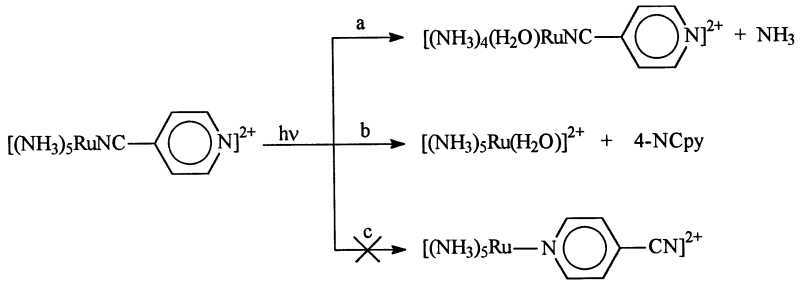

(5)

The linkage isomerization (Eq. 5c) does not occur under continuous photolysis. The results can be explained by the tuning model and according to their behavior these complexes can be classified as 'reactive'. Again, initial excitation into the ^{1}MLCT* manifold is followed by competitive internal conversion and intersystem crossing to the lowest energy ^{3}LF state or ^{3}LF manifold of excited states from which deactivation pathways lead to aquation products or the starting complex.

The 2-NCpy and 3-NCpy complexes have L photosubstitution quantum yields larger than those of ammonia, while for the 4-NCpy complex ammonia photoaquation quantum yield is higher. For Ru(II)–ammines ammonia photoaquation is in general the predominant photosubstitution reaction, but in some instances the opposite occurs. The reason for this different product ratio is unclear. However, these results suggest that the LEES responsible for the photochemistry observed should have more contribution from the z^2 orbital for 2-NCpy and 3-NCpy, while that of 4-NCpy would have more contribution from the $x^2 - y^2$ orbital.

Conceivably, a pyridinyl bonded complex, $[Ru(NH_3)_5(pyCN)]^{2+}$ could result from the LF photochemistry of the $[Ru(NH_3)_5(NCpy)]^{2+}$ (Eq. 5c). As for $[Ru(NH_3)_5(py)]^{2+}$, a η^2-bonded NCpy–Ru(II) intermediate could be formed, which for this case could eventually form the pyridinyl bonded linkage isomer, competitive with other decay routes. Similar intermediates were proposed to occur upon the reduction of the amido bonded $[(NH_3)_5Ru^{III}NHC(O)py]^{2+}$ to form the pyridinyl bonded $[(NH_3)_5Ru^{II}pyCONH_2]^{2+}$ ($pyCONH_2$ = nic or isn) [53]. More recently [54], both linkage isomerizations, amido to pyridinyl and pyridinyl to amido, were reported to occur for $[Ru(edta)(isn)]^{n-}$, with the same type of intermediate being inferred, as a possibility. For the cyanopyridine complexes, no such linkage isomer, $[Ru(NH_3)_5(pyCN)]^{2+}$ (Eq. 5c), was detected as a photoproduct [19]. However, this

does not rule out the possible existence of a η^2-bonded NCpy–Ru(II) intermediate, which could decay to other routes, without resulting in a linkage isomer [19].

3.2.3. Trans and cis-tetraammineruthenium(II) complexes with azines

3.2.3.1. Trans-[Ru(NH$_3$)$_4$LL′]$^{2+}$. (L = py; L′ = py, pz, or 4-acpy; L = L′ = pz) [21]. The presence of a second azine ligand in the *trans* position gives rise to two MLCT absorption bands, except for *trans*-[Ru(NH$_3$)$_4$(py)$_2$]$^{2+}$ [21,28]. The lower energy MLCT band (MLCT-1) has the higher absorptivity. Although less intense in all cases, the higher energy band (MLCT-2) is more prominent when L ≠ L′ [21,28]. For *trans*-[Ru(NH$_3$)$_4$(py)$_2$]$^{2+}$ the lowest energy LF absorption band should be close in energy to the MLCT band, and in the other cases it is in between MLCT-1 and MLCT-2. These complexes were irradiated with light corresponding to MLCT-1 and MLCT-2, and displayed photoaquation of ammonia, L, and L′ (Eq. 3) and the photochemical reactivity patterns could be described by the tuning model [21]. No distinctive feature was seen by irradiating at MLCT-2. However, for these complexes, the photoaquated ammonia are undoubtedly equatorial, and, thus, the LF excited state should have contribution from the $d_{x^2-y^2}$ orbital [21].

3.2.3.2. Cis-[Ru(NH$_3$)$_4$L$_2$]$^{2+}$. (L = py; 4-pic; isn; or 4-acpy) and *cis*-[Ru(NH$_3$)$_4$(isn)L]$^{2+}$ (L = py; 4-pic; pz; or 4-acpy) [24]. All of these complexes display two MLCT bands, as the *trans* complexes do, but for the *cis* complexes both are strong and generally overlap, resulting in a wide wavelength range for absorption in the visible range, the range being larger when the two azine ligands are different [24]. This also the case of other *cis*-[Ru(NH$_3$)$_4$LL′]$^{2+}$ (L and L′ = azine ligands) [34]. In these complexes, the obscured LF absorption bands are assumed to be near 390 nm, and, thus, three situations occur: (1) LF below both MLCTs; (2) LF above both MLCTs; and (3) LF in between MLCT-1 and MLCT-2. In contrast with the *trans* complexes, different d_π orbitals are involved in bonding with the azine ligands in each complex, as inferred from the oxidation potentials of the metallic center ($Ru^{2+/3+}$) data [34,35].

The wide range of absorption in the *cis* complexes allowed the study of the quantum yield dependence on irradiation wavelength in a larger number of irradiation wavelengths. These complexes show ammonia, L, and isn photoaquation (Eq. 3) and follow the tuning model. Irradiation of *cis*-[Ru(NH$_3$)$_4$(py)$_2$]$^{2+}$ and *cis*-[Ru(NH$_3$)$_4$(4-pic)$_2$]$^{2+}$ at 313, 365, 405 and 436 nm leads to irradiation wavelength independent and relatively high quantum yields of photosubstitution when compared to those of the other complexes, and these two ions were classified as 'reactive' complexes, while the others displayed irradiation wavelength dependent and relatively lower quantum yields of substitution, and were, classified as 'unreactive' [24]. With regard to the product distribution, the *cis*-[Ru(NH$_3$)$_4$(L)$_2$]$^{2+}$, *cis*-[Ru(NH$_3$)$_4$(isn)(4-acpy)]$^{2+}$, and *cis*-[Ru(NH$_3$)$_4$(isn)(pz)]$^{2+}$ complexes show ammonia photoaquation as the main reaction. Notably, for each *cis* complex, a fixed ratio of released ligands, independent of the irradiation wavelength is observed. Some exceptions were noted when very low quantum yields are involved, when the

experimental error is high [24]. The product distribution for the *cis*-$[Ru(NH_3)_4(isn)L]^{2+}$ complexes also showed that one of the unsaturated ligands is preferentially released [24]. The π-acceptor ability (and the synergistically increased σ-bonding) of the unsaturated ligands can be estimated to follow the order 4-pic < py < isn ca. pz < 4-acpy, as indicated by the decreasing energy of the lowest energy MLCT band [24]. For these *cis*-$[Ru(NH_3)_4(isn)L]^{2+}$ complexes there are three axes with different π-acceptor ability of the ligands. Ligands on the lower π-acceptor ability axes are preferentially labilized, and along an axis the weakest π-back-bonding ligand is aquated with the higher quantum yield [24]. The irradiation wavelength independent ratios of released ligands points to a common reactive excited state as the precursor to photosubstitution in each complex. Irradiation at higher energy states is followed by deactivation to one common reactive excited state, presumably a triplet ligand field excited state. No other distinctive feature is displayed by the presence of two MLCT bands in these complexes.

An exact description of the electronic configurations and states of these complexes is not simple, especially if one takes into account that the LF absorptions are not observed in the spectra. However, regardless of the number and exact descriptions of the ^{3}LF states, the results indicate a common excited state, or an ensemble of equilibrated excited states of the same electronic configuration, being responsible for the photosubstitution reactions observed [24]. Thus, the different ligand aquations for the different *cis* complexes reflect, in fact, different LF excited state electronic configurations, although one LF* state, or a manifold of equilibrated LF* states of the same electronic configuration, is the reactive state for each complex [24]. Perhaps, it should be examined theoretically how the ligands L affect the configurational mixing of lower energy LF states.

3.2.4. Trans-chlorocyclamruthenium(II) complexes with azines

3.2.4.1. Trans-[RuCl(cyclam)L]$^+$. (L = 4-pic; py; isn; or 4-acpy) [25]. These complexes with cyclam, which has a LF strength similar to that of four ammonias, show some similarities and some differences compared to other analogous ruthenium(II) ammines, especially the pentaammines [46,55]. The UV–vis spectra of aqueous solutions of the *trans*-$[RuCl(cyclam)L]^+$ complexes display single visible range MLCT and IL bands in the UV range, as do the corresponding pentaammines. However, between these two type of bands, the isn and 4-acpy complexes display a band of lower intensity assigned as LF [46]. The spectra of the py and 4-pic complexes do not show this band probably because it is obscured by the higher energy MLCT bands [46]. The energies of the MCLT bands and the $Ru^{III/II}$ redox potentials are essentially similar to those of the analogous pentaammines. However, the coordinated chloride turns out to be substitution inert, while the azine ligands aquate slowly [46].

The photochemical behavior of these complexes follows the tuning model [25]. Irradiation with light with energies in the MLCT range lead to exclusive azine aquation (Eq. (6)) at pH ca. 4.0, with the py and 4-pic complexes, with a LF* state as LEES, classified as 'reactive' and the isn and 4-acpy, with a MLCT* state as LEES, as 'unreactive'.

$$trans\text{-}[RuCl(cyclam)L]^{+} \xrightarrow[H_2O]{h\nu} trans\text{-}[RuCl(cyclam)(H_2O)]^{+} + L \quad (6)$$

The lowest energy LF* state configuration should have major contribution from the d_{z^2} orbital. Thus, population of this state would result in ligand labilization in the z axis. Eventual population of the $d_{x^2-y^2}$ orbital would lead to ligand labilization in the x and y axes, but since there is a macrocycle in the four coordination sites of these axes, no photosubstitution results.

The above situation is similar to that which occurs with *trans*-$[RhX_2(cyclam)]^{+}$ ($X = Cl^{-}$ or CN^{-}) complexes [56]. Irradiation in the lowest energy LF bands lead to luminescence, without photosubstitution reactions [56a], in the cyanide complex, and to chloride photoaquation, without luminescence, in the chloro complex [56a,56b]. This behavior was explained in terms of the LF* state electronic configuration. The complexes were assumed to have a D_{4h} symmetry, under which the lowest LF excited states would be a $^3A_{2g}$ for the cyanide complex and a ^3E_g for the chloro complex. Accordingly, for cyanide, the d_{z^2} orbital would be higher in energy than the $d_{x^2-y^2}$ orbital, and for the chloro it would be lower in energy. Thus, for the chloro complex the LF LEES would involve population of the z axis resulting in photosubstitution, while for the cyano complex, the LF LEES would involve population of the $d_{x^2-y^2}$ orbital, resulting in emission [56a]. Thus, for the *trans*-$[RuCl(cyclam)L]^{+}$ complexes, the results are consistent with the z axis being the weakest LF axis for the presence of the chloro ligand, and, hence, d_{z^2} orbital being lower in energy than the $d_{x^2-y^2}$ orbital.

The thermal substitution inertness of the chloro ligand was explained as a result of a combination of different factors, such as macrocyclic effect, a *trans* cooperative effect between the π-donor chloro and the π-acceptor azine through the Ru center involving a three-centered molecular orbital of π-symmetry, and the presence of hydrogen bonds between the chloro ligand and two of the cyclam nitrogen hydrogens [55]. These factors, and namely the hydrogen bonds, could also be present in the ^3E state responsible for the observed photochemistry, preventing the labilization of the chloride in the *trans*-$[RuCl(cyclam)L]^{+}$ complexes [25]. Since a ^3E is the state responsible for the photochemistry observed, then, the azine photoaquation should come not only for the population of the d_{z^2} orbital, but also from depopulation of the d_{xz} and d_{yz} orbitals, one of them being involved in the π-back-bonding between the Ru(II) and the azine [25].

3.2.5. Ru(II) ammine complexes with phosphites, phosphines, arsines, stibenes, carbonyl or H_2O ligands

3.2.5.1. Trans-$[Ru(NH_3)_4(P(III))L]^{2+}$. (P(III) = $P(OR)_3$, PR_3; L = $P(OR)_3$, PR_3; H_2O; CO) [22,26,27]. These complexes have some interesting properties [57] that made them suitable for the investigation of some photochemical reactions. The P(III) ligands are *trans* labilizing, and these complexes undergo thermal aquation of the ligand L (the aqua ligand was not examined), while the ammonias are substitution inert (Eq. 7).

$$trans\text{-}[Ru(NH_3)_4(P(III)L]^{2+} \xrightarrow{H_2O} \begin{cases} \rightarrow trans\text{-}[Ru(NH_3)_4(P(III)(H_2O)]^{2+} + L \\ \not\rightarrow trans\text{-}[Ru(NH_3)_3(H_2O)(P(III)L]^{2+} + NH_3 \end{cases} \quad (7)$$

These complexes have high $Ru^{II/III}$ oxidation potentials, the P(III) ligands are of high ligand field strength, and thus, z axis (P(III)RuL) is the higher ligand field strength axis. In addition, these complexes display LF bands as the lowest energy absorption bands in the UV–vis spectra (Table 5) (owing to the high $Ru^{II/III}$ oxidation potential). In contrast with the ruthenium ammine complexes with azines, there are no MLCT bands obscuring the LF bands which are responsible for the photosubstitution reactions in Ru(II) ammines. And, furthermore, there are no low lying CTTS states. Thus, the photochemical behavior could be more easily related with the LF spectra in these P(III) complexes. The *trans*-$[Ru(NH_3)_4(P(III))L]^{2+}$ complexes have lowest energy absorption in the UV–vis spectra, which upon deconvolution, reveal two LF bands. For the *trans*-$[Ru(NH_3)_4(P(III))_2]^{2+}$ complexes they were assigned to $^1A_{1g} \rightarrow {}^1E_g$ ($\lambda_{max} = 294–297$ nm) and $^1A_{1g} \rightarrow {}^1A_{2g}$ ($\lambda_{max} = 359–360$ nm), and $^1A_1 \rightarrow {}^1E$ ($\lambda_{max} = 298–329$ nm) and $^1A_1 \rightarrow {}^1A_2$ ($\lambda_{max} = 370–392$ nm) for the *trans*-$[Ru(NH_3)_4(P(III))L]^{2+}$ complexes. The ^1E component, higher in energy, involves a transition from (xz, yz) to z^2, while the A_2 component involves an xy to $x^2 - y^2$ transition. Eighteen such complexes had their photochemical properties examined, and notably, excitation to the LEES LF, i.e. $^1A_2$ or $^1A_{2g}$ results in exclusive ammonia photoaquation in all of these complexes, while excitation into the ^1E or ^1E_g results in P(III) and ammonia photoaquation in *trans*-$[Ru(NH_3)_4(P(III))_2]^{2+}$, and CO and ammonia photoaquation for *trans*-$[Ru(NH_3)_4(P(III)L]^{2+}$ (L = CO, or H_2O) (Eq. 8).

$$trans\text{-}[Ru(NH_3)_4(P(III))L]^{2+} \xrightarrow{h\nu} \begin{cases} \xrightarrow{a} trans\text{-}[Ru(NH_3)_4(P(III))(H_2O)]^{2+} + L \\ \xrightarrow{b} trans\text{-}[Ru(NH_3)_3(H_2O)(P(III))L]^{2+} + NH_3 \end{cases} \quad (8)$$

The photochemical behavior of these complexes also show other interesting features. The ammonia photoaquation quantum yields are very similar for all complexes (ϕ ca. 3) for excitation into ^1E or ^1E_g and into $^1A_2$ or $^1A_{2g}$; however, no correlation between the cone angle of the P(III) ligand, which ranged from 107 to 172°, and the quantum yields could be set, and, as a matter of fact, the observed similarity of the ϕ values for ligands with quite different cone angle values suggests that steric effects can be neglected in these photosubstitution reactions.

The absence of P(III) labilization upon irradiation at 360–370 nm, where ammonia aquation occurs, implies that the z^2 orbital is not contributing to the LEES, which should have contribution from the $d_{x^2-y^2}$ orbital. Thus, labilization of P(III) with light of 313 nm should then arise from reactions of upper energy excited states competitive with other deactivation pathways. Initial excitation, with light of 360–370 nm, to a $^1A_2$ or $^1A_{2g}$ state is followed by efficient intersystem crossing to a $^3A_2$ or $^3A_{2g}$ from which exclusive ammonia aquation occurs. Irradiation with light of 313 nm results in a ^1E or ^1E_g excited state, followed by intersystem crossing to lower energy excited states, the lowest of which is $^3A_2$ or $^3A_{2g}$. The

P(III) labilization should arise from a ^3E or ^3E_g state between ^1E or ^1E_g and $^1A_2$ or $^1A_{2g}$. Since irradiation at 360–370 nm does not result in P(III) labilization, then the ^3E or ^3E_g state should lie above or near $^1A_2$ or $^1A_{2g}$. Conceivably, according to these results, it is possible to design the synthesis of species involving substitution in the equatorial position, which, in the case of P(III) complexes, are very inert.

Analysis of the photochemical behavior of the *trans*-$[Ru(NH_3)_4(P(OEt)_3)CO]^{2+}$ complexes reveals interesting points. Based on $Ru^{II/III}$ oxidation potentials of *trans*-$[Ru(NH_3)_4(P(OEt)_3)(H_2O)^{2+}$ and *trans*-$[Ru(NH_3)_5CO]^{2+}$, it was inferred that CO stabilizes Ru(II) through back-bonding more than $P(OEt)_3$ does. Triethylphosphite is a moderate σ base and a strong π-acceptor, while CO is a poor σ-donor and a strong π-acceptor, and, thus, even considering the synergistic effect of π-backbonding on σ-bonding, the Ru(II)–CO bond would be mainly a π-bonding. For *trans*-$[Ru(NH_3)_4(P(OEt)_3)CO]^{2+}$ irradiation into the $^1A_2$ state results in exclusive ammonia aquation, while irradiation into the ^1E state leads to CO aquation but no phosphite aquation [26,58]. This would be in apparent contrast with the behavior of the *cis*-$[Ru(NH_3)_4(isn)L]^{2+}$ complexes [24], for which the ligands of lower π-backbonding ability are more easily labilized. In these *cis* complexes the depopulation of a nonbonding d_π orbital and population of a σ* orbital would not involve backbonding breaking, and, thus, the weaker π-backbonding ligand will be the more easily labilized. The apparent contradiction for *trans*-$[Ru(NH_3)_4(P(OEt)_3)CO]^{2+}$ was cleared by analysis of the nature of the bonds involved in the reactions. The E state involves a (*xz*, *yz*) to z^2 transition, i.e. depopulation of orbitals which are involved in backbonding to an antibonding orbital along the *z* axis. Since CO is mostly bonded through π-backbonding, then depopulation of *xz*, *yz* orbitals affects the CO ligand more, resulting in CO aquation rather than $(P(OEt)_3)$.

The *trans*-$[Ru(NH_3)_4(P(III))(H_2O)]^{2+}$ complexes luminesce at room temperature, with an emission maximum around 408 nm; it was argued that the biexponential decay of the luminescence could be due to an interconversion process between the $^1E_1$ and $^1A_2$ excited states prior to deactivation to the ground state [59]. For the *trans*-$[Ru(NH_3)_4(P(OC_4H_9)_3)(H_2O)]^{2+}$ complex, the energy difference between these two states is in between 17 and 25 kJ mol^{-1} [59]. Furthermore, *trans*-$[Ru(NH_3)_4((P(OR)_3)_2]^{2+}$ complexes quench the Tb^{3+} luminescence (emission at 488 and 545 nm) by a collisional energy transfer, with rate constants in the range 1.1–3.3 ($\times 10^6$) M^{-1} s^{-1}; the rate constants decrease with increasing size of the substituents in the phosphane ligand.

Ammonia aquation with a quantum yield of 0.32 is also the result of the irradiation of *trans*-$[Ru(NH_3)_4(TPAH)(H_2O)]^{3+}$, which has LF bands as lower energy bands, with light of wavelength 310 and 370 nm [60].

3.2.5.2. $[Ru(NH_3)_5(CO)]^{2+}$ and trans-$[Ru(NH_3)_4(H_2O)(CO)]^{2+}$ [26,58]. These complexes have LF bands as lowest energy bands (λ_{max} ca. 365 nm) and higher energy LF bands with some CTTS character. The photochemical behavior resembles that of the $[Ru(NH_3)_5(acn)]^{2+}$ complex. Irradiation with light of 365 nm results in exclusive photosubstitution of the ammine and carbonyl ligands, while irradiation

with light of 313 or 254 nm leads to both photosubstitution and photoredox processes.

3.2.5.3. $[Ru(NH_3)_5L]^{2+}$. ($L = P(Ph)_3$, $As(Ph)_3$, $Sb(Ph)_3$) [26,61]. These complexes show LF bands as lowest energy bands and their irradiation leads to photosubstitution reactions of the ammine and L ligands.

3.2.6. Energies of the excited state precursor to the photochemistry

The obscured ^{1}LF absorption bands in ammineruthenium(II) complexes with pyridines and similar ligands had their energies estimated by calculations and analogies with related systems [38–43,62]. In addition, for these Ru(II) complexes there are no reports of observed ^{3}LF bands in the spectra. As described above, ^{3}LF states are assigned to be the precursors of the observed photosubstitution reactions in these Ru(II) complexes. However, recently, a series of Ru(II) complexes have had the energies of the reactive excited state determined [19b,62–64]. The energies of the reactive excited states of $[Ru(NH_3)_5(py)]^{2+}$ [62], $[Ru(NH_3)_6]^{2+}$ [63], $[Ru(NH_3)_5(2\text{-}NCpy)]^{2+}$ [19b], $[Ru(NH_3)_5(3\text{-}NCpy)]^{2+}$ [19b], *trans*-$[RuCl(cyclam)(4\text{-}pic)]^{2+}$ [19b] and *trans*-$[RuCl(cyclam)(py)]^{2+}$ [19b] were determined by sensitization and quenching of their excited states using a series of singlet and triplet dyes.

3.2.6.1. $[Ru(NH_3)_5(py)]^{2+}$ [62]. Sensitization of the complex with ^{3}Biacetyl, ^{1}Safranine-T, and ^{1}Rhodamine-B lead to their luminescence quenching and to a photochemical behavior identical to that observed by direct irradiation of the complex, with the same photoproducts, quantum yields, and products ratios. However, the photochemical reactions of the complex are quenched by Neutral Red. The observed quenching of the dyes and sensitization of the complex results from an electronic energy transfer process, through a long-range resonance Förster energy transfer mechanism, which is not limited by spin conservation rules. However, quenching of both triplet or singlet luminescences of the dyes could also be explained by an heavy atom effect exercised by Ru. The results indicate that the excited state or manifold of excited states precursor of the observed photoaquation in the complex lies in the energy range between 17 000 and 17 700 cm^{-1}. However, due to the proximity of the energies of the MLCT and LF states in this complex, it is practically impossible to populate one of these selectively. Therefore, there may be some doubt whether the acceptor state in the sensitized reactions has MLCT or LF character. However, considering the general photoreactivity of Ru(II) ammines, the reactive excited state should have LF character. The ^{3}LF energy was calculated as 17 700 cm^{-1} using estimated LF and Racah parameters for $Ru(NH_3)_6^{2+}$ [39,42], while the ^{3}MLCT was estimated as 19 000 cm^{-1} [17], The energy range determined of $17\,000 - 17\,700$ cm^{-1} is in close agreement with the estimated and calculated values for this complex.

3.2.6.2. $Ru(NH_3)_6^{2+}$ [63]. The behavior of this complex is similar to that of $[Ru(NH_3)_5(py)]^{2+}$ upon sensitization of the complex with ^{3}Biacetyl, ^{1}Safranine-T, and ^{1}Rhodamine-B and quenching by Neutral Red. In this case, the LEES is a LF

state, which leads to photosubstitution, with an upper energy CTTS state, which leads to photooxidation. The excited state or manifold of excited states precursor of the observed photoaquation in this complex lies in the energy range, 16 900–17 700 cm^{-1}, identical to that of $[Ru(NH_3)_5(py)]^{2+}$. This similarity has been taken as indicative that back-bonding in $[Ru(NH_3)_5(py)]^{2+}$ is not important enough to result in large splitting of the LF states.

3.2.6.3. $[Ru(NH_3)_5(2\text{-}NCpy)]^{2+}$ and $[Ru(NH_3)_5(3\text{-}NCpy)]^{2+}$ [19b,64]. The sensitization and quenching experiments with those complexes indicated that the energy of the excited states (or manifold excited states) precursor of the photosubstitution reactions observed lie between 15 300 and 16 200 cm^{-1} [19b,64].

3.2.6.4. Trans-[RuCl(cyclam)(4-pic)]$^{2+}$, and trans-[RuCl(cyclam)(py)]$^{2+}$ [19b,64]. The sensitization and quenching experiments with those complexes showed up that the energy of the excited states (or manifold excited states) precursor of the photosubstitution reactions observed lie between 16 200 and 16 900 cm^{-1} [19b,64].

3.2.7. Ru(II) ammine complexes with nitrosyl

The importance of nitric oxide and related species is well known nowadays, and it forms more complexes with ruthenium than with any other metal [2,65]. Although many complexes of Ru with nitric oxide are known, including ammines, several studies need to be done in view of the role of nitric oxide in different processes, especially biological. This is one of the current research topics in our laboratory, which studies ruthenium amine complexes with nitric oxide and related species to understand their properties, aiming to design controlled NO releasers or scavenger complexes. In particular, one of the targets is to study the photochemical release of NO.

Ruthenium(II) ammines with nitrosyl show UV–vis spectra quite different from those of complexes with other unsaturated ligands such as pyridines [66]. Only weak absorptions are seen in the visible range (λ_{max} ca. 400–500 nm; ε ca. < 50 mol^{-1} l cm^{-1}) [23], along with stronger bands at higher energy. As described above, for Ru(II)ammines with unsaturated ligands, only photosubstitution reactions result primarily from the lowest energy excited states; eventual photoredox processes occur upon irradiation at higher energies for some complexes which display higher energy bands with some CTTS character. In contrast, preliminary results with some *trans*-$[Ru(NO)(NH_3)_4(py\text{-}X)]^{3+}$ complexes showed that irradiation with light of 335 nm resulted notably in free NO^0 and *trans*-$[Ru(NH_3)_4(py\text{-}X)(H_2O)]^{3+}$, as indicated by the following equation:

$$trans\text{-}[Ru^{II}(NO)(NH_3)_4L]^{3+} \xrightarrow{h\nu} trans\text{-}[Ru^{III}(NH_3)(H_2O)L]^{3+} + H_2O$$

In contrast, irradiation with light of 436 nm did not result in any observable photoreaction [23]. However, the experimental conditions did not rule out a possible ammonia aquation at lower energy, which should be investigated. Although a preliminary assignment was made to explain the photoredox process, its origin is unclear. Similar reactions were reported to occur for the

$[Ru(NO)(NH_3)_5)]^{3+}$ complex with different counter-ions [67]; the authors claim an outer-sphere redox process between the cation and anion, resulting in $[Ru(OH)(NH_3)_5]^{2+}$ and NO^0. The ruthenium(II) ammine complexes with nitrosyl show two distinctive features: a release of nitric oxide, which is of the utmost importance in view of potential applications, and a markedly different photochemical behavior; these are currently under investigation in our laboratory.

Acknowledgements

The author acknowledges the support of FAPESP, FINEP, CAPES, CNPq, and CAPES/PADCT and CNPq/PADCT for the research developed in this laboratory and research fellowship from CNPq. The author also thanks Professor Peter C. Ford for reading the manuscript.

References

[1] A.D. Allen, C.V. Senoff, J. Chem. Soc. Chem. Commun. (1965) 621.
[2] E.A. Seddon, K.R. Seddon, The Chemistry of Ruthenium, Elsevier, Amsterdam, 1984.
[3] (a) J.F. Endicott, H. Taube, J. Am. Chem. Soc. 84 (1962) 4984. (b) J.F. Endicott, H. Taube, J. Am. Chem. Soc. 86 (1964) 1686. (c) J.F. Endicott, H. Taube, Inorg. Chem. 4 (1965) 437.
[4] V. Balzani, V. Carassiti, Photochemistry of Coordination Compounds, Academic Press, London, 1970.
[5] (a) P.C. Ford, D.H. Stuermer, D.P. McDonald, J. Am. Chem. Soc. 91 (1969) 6209. (b) P.C. Ford, D.A. Chaisson, D.H. Stuermer, J. Chem. Soc. Chem. Commun. (1971) 530. (c) D.A. Chaisson, R.E. Hintze, D.H. Stuermer, J.D. Petersen, D.P. McDonald, P.C. Ford, J. Am. Chem. Soc. 94 (1972) 6665.
[6] (a) V. Balzani, A. Juris, M. Venturi, S. Campagna, S. Serroni, Chem. Rev. 96 (1996) 759. (b) A. Juris, V. Balzani, F. Barigeletti, S. Campagna, P. Belser, A. von Zelewsky, Coord. Chem. Rev. 84 (1988) 85. (c) C.A. Bignozzi, R. Argazzi, C. Chiorboli, S. Roffia, F. Scandola, Coord. Chem. Rev. 111 (1991) 261. (d) F. Scandola, M.T. Indelli, C. Chiorboli, C.A. Bignozzi, Top. Curr. Chem. 158 (1990) 73. (e) J.R. Schoonover, C.A. Bognozzi, T.J. Meyer, Coord. Chem. Rev. 165 (1997) 239. (f) K. Kalyanasundaram, Coord. Chem. Rev. 46 (1982) 159. (g) K. Kalyanasundaram, Photochemistry of Polypyridine and Porphirin Complexes, Academic Press, New York, 1992.
[7] (a) V. Balzani, F. Scandola, Supramolecular Photochemistry, Ellis Horwood, Chichester, UK, 1991. (b) V. Balzani, R. Ballardini, F. Bolletta, M.T. Gandolfi, A. Juris, M. Maestri, M.F. Manfrin, M.L. Moggi, N. Sabbatini, Coord. Chem. Rev. 125 (1993) 75. (c) V. Balzani, Tetrahedron 48 (1992) 10 443.
[8] P.C. Ford, J.D. Petersen, R.E. Hintze, Coord. Chem. Rev. 14 (1974) 67.
[9] P.C. Ford, R.E. Hintze, J.D. Petersen, in: A.W. Adamson, P.D. Fleischauer (Eds.), Concepts of Inorganic Photochemistry, Wiley, New York, 1975 (Chapter 5).
[10] P.C. Ford, G. Malouf, J.D. Petersen, V.A. Durante, ACS Adv. Chem. 150 (1976) 187.
[11] P.C. Ford, ACS Adv. Chem. 168 (1978) 73.
[12] P.C. Ford, Rev. Chem. Interm. 2 (1979) 267.
[13] P.C. Ford, D. Wink, J. Dibenedetto, Prog. Inorg. Chem. 30 (1983) 213.
[14] P.C. Ford, DeF.P. Rudd, R. Gaunder, H. Taube, J. Am. Chem. Soc. 90 (1968) 1187.
[15] (a) H.E. Toma, D.Sc. Thesis, Instituto de Química, Universidade de São Paulo, Brazil, 1974. (b) H.E. Toma, J.M. Malin, J. Am. Chem. Soc. 94 (1972) 4039.
[16] C. Creutz, M.H. Chou, Inorg. Chem. 26 (1987) 2995.

[17] J.R. Winkler, T.L. Netzel, C. Creutz, N. Sutin, J. Am. Chem. Soc. 109 (1987) 2381.
[18] (a) G. Malouf, P.C. Ford, J. Am. Chem. Soc. 99 (1977) 7213. (b) G. Malouf, Ph.D. Thesis, University of California, Santa Barbara, CA, USA, 1977.
[19] (a) M. Silva, E. Tfouni, J. Photochem. Photobiol. A, 122 (1999) 103. (b) M. Silva, D.Sc. Thesis, Instituto de Química de São Carlos, Universidade de São Paulo, Brazil, 1997.
[20] R.E. Hintze, P.C. Ford, J. Am. Chem. Soc. 97 (1975) 2664.
[21] E. Tfouni, P.C. Ford, Inorg. Chem. 19 (1980) 72.
[22] E.E. Mazzetto, E. Tfouni, D.W. Franco, Inorg. Chem. 35 (1996) 3513.
[23] M.C. Gomes, C.U. Davanzo, S.C. Silva, L.G.F. Lopes, P.S. Santos, D.W. Franco, J. Chem. Soc. Dalton Trans. (1998) 601.
[24] L.A. Pavanin, Z.N. Rocha, E. Giesbrecht, E. Tfouni, Inorg. Chem. 30 (1991) 2185.
[25] M. Silva, E. Tfouni, Inorg. Chem. 36 (1997) 274.
[26] L.M.A. Plicas, D.Sc. Thesis, Instituto de Química de São Carlos, Universidade de São Paulo, Brazil, 1995.
[27] S.E. Mazzetto, L.M.A. Plicas, E. Tfouni, D.W. Franco, Inorg. Chem. 31 (1992) 516.
[28] M.L. Bento, E. Tfouni, Inorg. Chem. 27 (1988) 3410.
[29] R.E. Clarke, P.C. Ford, Inorg. Chem. 9 (1970) 227.
[30] P.C. Ford, Coord. Chem. Rev. 5 (1970) 75.
[31] J.C. Curtis, P.B. Sullivan, T.J. Meyer, Inorg. Chem. 22 (1983) 224.
[32] C. Creutz, N. Sutin, Inorg. Chem. 15 (1976) 496.
[33] V.A. Durante, P.C. Ford, Inorg. Chem. 18 (1979) 588.
[34] L.A. Pavanin, D.Sc. Thesis, Instituto de Química da Universidade de São Paulo, Brazil, 1988.
[35] L.A. Pavanin, E. Giesbrecht, E. Tfouni, Inorg. Chem. 24 (1985) 4444.
[36] (a) V.E. Alvarez, R.J. Allen, T. Matsubara, P.C. Ford, J. Am. Chem. Soc. 96 (1974) 7686. (b) V.E. Alvarez, Ph.D. Thesis, University of California, Santa Barbara, CA, USA, 1974.
[37] A.S.A.T. Paula, B.E. Mann, E. Tfouni, Polyhedron 18 (1999) 2017.
[38] H.H. Schmidtke, D. Garthoff, Helv. Chim. Acta 49 (1966) 2039.
[39] T. Matsubara, S. Efrima, H.I. Metiu, P.C. Ford, J. Chem. Soc. Faraday Trans. II 75 (1979) 390.
[40] A.W. Adamson, A.H. Sporer, J. Am. Chem. Soc. 80 (1958) 3865.
[41] F. Nordmeyer, H. Taube, J. Am. Chem. Soc. 90 (1968) 1162.
[42] J.D. Petersen, R.J. Watts, P.C. Ford, J. Am. Chem. Soc. 98 (1976) 3188.
[43] R.J. Balahura, Can. J. Chem. 52 (1974) 1762.
[44] J.F.F. Alves, A.M.G. Plepis, C.U. Davanzo, D.W. Franco, Polyhedron 12 (1993) 2215.
[45] W. Caetano, J.F.F. Alves, B.S. Lima Neto, D.W. Franco, Polyhedron 14 (1995) 1295.
[46] R.S. Silva, E. Tfouni, Inorg. Chem. 31 (1992) 3313.
[47] C. Sigwart, J. Spence, J. Am. Chem. Soc. 91 (1969) 3991.
[48] T. Matsubara, P.C. Ford, Inorg. Chem. 17 (1978) 1747.
[49] J.H. Baxendale, Q.G. Mulazzani, J. Inorg. Nucl. Chem. 33 (1971) 823.
[50] D.A. Chaisson, M.A. Dissertation, University of California, Santa Barbara, CA, USA, 1971.
[51] (a) M.S. Wrighton, H.B. Abrahamson, D.L. Morse, J. Am. Chem. Soc. 98 (1976) 4105. (b) H.B. Abrahamson, M.S. Wrighton, Inorg. Chem. 17 (1978) 3385. (c) J.E. Figard, J.D. Petersen, Inorg. Chem. 17 (1978) 1059.
[52] R.E. Hintze, Ph.D. Thesis, University of California, Santa Barbara, CA, USA, 1974.
[53] M.H. Chou, B.S. Brunschwig, C. Creutz, N. Sutin, A. Yeh, R.C. Chang, C.T. Lin, Inorg. Chem. 31 (1992) 5347.
[54] D. Chatterjee, H.C. Bajaj, J. Chem. Soc. Dalton Trans. (1995) 3415.
[55] R.S. Silva, M.T.P. Gambardella, R.H.A. Santos, B.E. Mann, E. Tfouni, Inorg. Chim. Acta 245 (1996) 215.
[56] (a) D.B. Miller, P.K. Miller, N.A.P. Kane-Maguire, Inorg. Chem. 22 (1983) 3831. (b) C. Kutal, A.W. Adamson, Inorg. Chem. 12 (1973) 1454. (c) L.J. McClure, P.C. Ford, J. Phys. Chem. 96 (1992) 6640.
[57] (a) D.W. Franco, H. Taube, Inorg. Chem. 17 (1978) 571. (b) J.C. Nascimento Filho, J.M. Rezende, B.S. Lima Neto, D.W. Franco, Inorg. Chim. Acta 145 (1988) 111. (c) R.L. Sernaglia, D.W. Franco, Inorg. Chem. 28 (1989) 3485 and Refs. therein. (d) D.W. Franco, Inorg. Chim. Acta 48 (1981) 1. (e) D.W. Franco, Coord. Chem. Rev. 119 (1992) 199.

[58] L.M.A. Plicas, D.W. Franco, E. Tfouni, in preparation.
[59] S.E. Mazzetto, M.H. Gehlen, D.W. Franco, Inorg. Chim. Acta 254 (1997) 79.
[60] P.M. Frugeri, L.C.G. Vasconcellos, S.E. Mazzetto, D.W. Franco, New J. Chem. 21 (1997) 349.
[61] L.M.A. Plicas, E. Tfouni, in preparation.
[62] R.M. Carlos, M.G. Neumann, E. Tfouni, Inorg. Chem. 35 (1996) 2229.
[63] R.M. Carlos, E. Tfouni, M.G. Neumann, J. Photochem. Photobiol. A 103 (1997) 121.
[64] M. Silva, E. Tfouni, in preparation.
[65] (a) F. Bottomley, Coord. Chem. Rev. 26 (1978) 7. (b) G.B. Richter-Addo, P. Legzdins, Metal Nitrosyls, Oxford University Press, New York, 1992. (c) L. Packer (Ed.), Methods in Enzimology. Nitric oxide, vol. 268, Academic Press, San Diego, 1996.
[66] C.W.B. Bezerra, M.G. Gomes, S.C. Silva, M.T.P. Gambardella, R.H.A. Santos, L.M.A. Plicas, E. Tfouni, D.W. Franco, Inorg. Chem. 1999 (in press).
[67] A.B. Nikolski, V.Y. Kotov, Vestn. Lenin U. Fiz. Kh. 3 (1986) 54.